

# **REDUCTION OF MUTUAL COUPLING FOR MIMO ANTENNA**

## **A PROJECT REPORT**

**Submitted by**

**JEEVA. R**

**PRANAV. P.B**

**RAMEEZFATHIMA. S**

**SELVA SEJIN. M**

**in partial fulfilment for the award of the degree**

**of**

**BACHELOR OF ENGINEERING**

**in**

**ELECTRONICS AND COMMUNICATION ENGINEERING**

**COIMBATORE INSTITUTE OF ENGINEERING AND TECHNOLOGY**



**Autonomous /Approved by AICTE/  
Affiliated to Anna University  
Accredited by NAAC with “A” Grade  
COIMBATORE-641109**



**JUNE 2022**

**COIMBATORE INSTITUTE OF ENGINEERING AND TECHNOLOGY**  
**(Autonomous/Approved by AICTE/Affiliated to Anna University)**  
**COIMBATORE-641109**

**BONAFIDE CERTIFICATE**

Certified that this project report "**REDUCTION OF MUTUAL COUPLING FOR MIMO ANTENNA**" is the bonafide work of

<b>JEEVA. R</b>	<b>710518106004</b>
<b>PRANAV. P.B</b>	<b>710518106010</b>
<b>RAMEEZFATHIMA. S</b>	<b>710518106012</b>
<b>SELVA SEJIN. M</b>	<b>710518106015</b>

who carried out the project work under my supervision.

**SIGNATURE**

**Dr. K. KALAMANI., M.E., Ph.D.  
HEAD OF THE DEPARTMENT**

Department of Electronics and  
Communication Engineering  
Coimbatore Institute of Engineering and  
Technology,  
Coimbatore 641 109

**SIGNATURE**

**Ms. R. GAYATHRI., M.E.,  
ASSISTANT PROFESSOR**

Department of Electronics and  
Communication Engineering  
Coimbatore Institute of Engineering and  
Technology,  
Coimbatore 641 109

Submitted for the University Project Viva-Voce held on \_\_\_\_\_

**Internal Examiner**

**External Examiner**

## **ACKNOWLEDGEMENT**

Our heart is filled with gratitude to Almighty God for empowering me with the courage, wisdom and strength to carry out this project work successfully.

We would like to record our sincere indebtedness and gratitude to our renowned Director, **Dr. K.A. Chinnaraju, M.Sc., M.B.A., Ph.D.**, for his noteworthy efforts to enhance our professional dexterity and co-curricular excellence.

We indebted to our respected Principal, **Dr. N. Nagarajan, M.E., Ph.D.**, for providing us with necessary facilities to carry out our project work.

We express our sincere thanks to our Head of the Department, **Dr. K. Kalamani., M.E., Ph.D.**, for her timely help and co-ordinate and also we wish to express our sincere thanks to our Project Coordinator **Mr. K. Yogeshvaran, M.E.**, Department of Electronics and Communication, for his support in caring out this project.

We are very much pleased to acknowledge our sincere thanks to our guide **Ms. R. Gayathri., M.E.**, for her guidance and valuable suggestions.

Finally, we extend our thanks to the management, faculty members, parents and our student friends for their support and encouragement.

## **ABSTRACT**

Wireless communication is the transfer of information between two or more points that do not use an electrical conductor as a medium for the transfer. Antenna array are inevitable component in any microwave communication system that demands large coverage. Multiple-input multiple-output MIMO technology has been attracting extensive attention in wireless communications, owing to its advanced characteristics of high channel capacity and spectrum efficiency. The replication of identical antenna elements improves the overall radiation performance for long distance communication. However, for a size-constraint MIMO device with physical limitation for antennas installation, the service performance is always degraded by the interferences through mutual couplings among antenna elements. This mutual coupling performance degradation can be overcome by isolation enhancement. To achieve isolation enhancement, the use of electromagnetic bandgap (EBG) structures, defected grounded structures (DGS), meta-materials, split ring and complementary split ring resonators (SRR & CSRR) can be used. In this project, the design of improved dual-layer mushroom (IDLM) and back-to-back E-shaped stubs for mutual coupling reduction between microstrip patch antennas. The antenna is studied from the aspects of isolation, return loss, current and electric field distribution, radiation pattern, and diversity performance in a frequency range of 2.45 GHz of return loss -9.327dB, gain 3.62914 ,directivity 6.11762, isolation -54.342dB.

## TABLE OF CONTENTS

CHAPTERNO.	TITLE	PAGE NO.
	<b>ABSTRACT</b>	iv
	<b>LIST OF TABLES</b>	vii
	<b>LIST OF FIGURES</b>	viii
	<b>LIST OF ABBREVIATIONS</b>	ix
<b>1</b>	<b>INTRODUCTION</b>	<b>1</b>
	1.1 ANTENNAS	1
	1.2 TYPES OF ANTENNA	2
	1.3 MICROSTRIP PATCH ANTENNA	3
	1.3.1 Advantages	4
	1.3.2 Applications	4
	1.4 FEEDING TECHNIQUES	4
	1.4.1 Microstrip line feed	5
	1.4.2 Coaxial probe feed	5
	1.4.3 Proximity coupled feed	6
	1.4.4 Aperture coupled feed	6
	1.5 MIMO ANTENNA	7
	1.6 MUTUAL COUPLING	7
	1.7 DUAL LAYER MUSHROOMSTRUCTURE	8
	1.8 E-SHAPED STRUB	9
	1.9 ADVANTAGE	10
	1.10 APPLICATION	10
<b>2</b>	<b>LITERATURE SURVEY</b>	<b>11</b>
<b>3</b>	<b>ANTENNA DESIGN AND ANALYSIS</b>	<b>18</b>
	3.1 OVERVIEW	18
	3.2 STRUCTURE OF ANTENNA	19
	3.3 COUPLING REDUCTION PERFORMANCE	21
	3.4 SUBSTRATE MATERIAL	24
	3.5 APPLICATION OF ANTENNA	25

<b>4</b>	<b>RESULTS AND DISCUSSIONS</b>	<b>26</b>
4.1	ADS	26
4.1.1	KEY FEATURES	26
4.2	DESIGN LAYOUT OF PROPOSED MODEL	27
4.3	PERFORMANCE ANALYSIS	27
4.4	EXPERIMENTAL RESULT AND DISCUSSION	27
4.4.1	ANTENNA PERFORMANCE	27
4.4.2	DIVERSITY ANALYSIS	30
4.5	SIMULATED RESULT	32
4.5.1	Return loss	32
4.5.2	Isolation	32
4.5.3	Insertion loss	33
4.5.4	Gain	33
4.5.5	Axial ratio	34
4.5.6	Radiation Pattern	34
<b>5</b>	<b>CONCLUSION</b>	<b>35</b>
	<b>REFERENCES</b>	<b>36</b>

## LIST OF TABLES

<b>TABLE NO.</b>	<b>TITLE</b>	<b>PAGE NO.</b>
1	Dimensions of optimized parameters of the proposed system	20
2	FR-4 Specification	24
3	Dimension of optimized parameters of the proposed antenna	30

## **LIST OF FIGURES**

<b>FIGURE NO</b>	<b>TITLE</b>	<b>PAGENO.</b>
1.1	Antenna	1
1.2	Microstrip Patch Antenna	3
1.3	Microstrip line feed	5
1.4	Coaxial probe feed	5
1.5	Proximity coupled feed	6
1.6	Aperture coupler feed	6
1.7	MIMO	7
1.8	Mutual coupling	8
1.9	EBG Structure	9
1.10	E-Shaped stub	9
3.1	Coaxial probe	19
3.2	a) Geometry of the proposed antenna b) Dual layer mushroom	19 20
3.3	Configuration of Ant 1, Ant 2 and Ant 3	22
3.4	Electric field distribution:(a)At1;At3	23
4.1	Model of patch with feed	27
4.2	Simulated and measurement S-parameter	28
4.3	Simulation and measurement far-field	29
4.4	Gain and Efficiency	29
4.5	Return loss	32
4.6	Isolation loss measurement	32
4.7	Measurement of insertion loss in dB	33
4.8	Gain pattern of proposed model	33
4.9	Axial Ratio of the proposed model	34
4.10	Radiation pattern of the proposed model	34

## **LIST OF ABBREVIATION**

DGS	Defected Ground Structure
SRR	Split-ring Resonator
CSRR	Concentric complementary Split Ring Resonator
EM	Electromagnetic
MIMO	Multiple Input Multiple Output
MC	Mutual Coupling
IDLM	Improved Dual Layer Mushroom
ECC	Envelope Correlation Coefficient
EBG	Electromagnetic band-gap
TARC	Total Active Reflection Coefficient
DG	Diversity Gain
FR4	Flame Retardant 4
AT	Antenna
PIFA	Planar inverted-F antenna
ADS	Advanced Design System

# CHAPTER 1

## INTRODUCTION

### 1.1 Antennas

An antenna is defined as “a usually metallic device for radiating or receiving radio waves”. Antennas play a major role in the wireless communication systems. The performance of antenna systems can significantly enhance the performance of wireless communication systems. For some applications, the single element antenna is unsuitable because it does not meet the required gain and radiation patterns. A signal from a transmission line or the guiding device like a co-axial cable, is given to an antenna, which then converts the signal into electromagnetic energy to be transmitted through space. There are many techniques implemented to increase the antenna performance such as

- SISO (Single Input Single Output)
- MISO (Multiple Input Single Output),
- SIMO (Single Input Multiple Output)
- MIMO (Multiple Input Multiple Output)

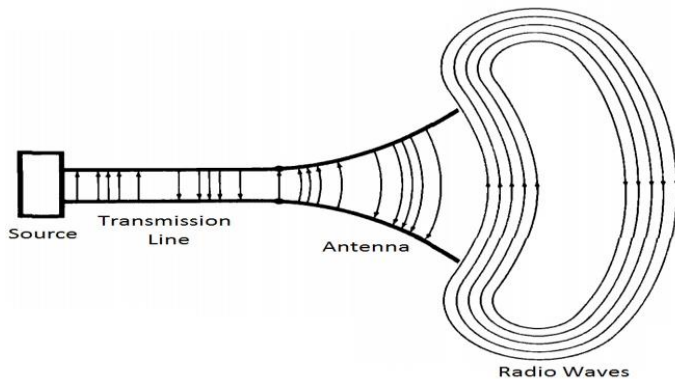


**Fig 1.1 Antenna**

Fig. 1.1 shows the Electromagnetic waves are often referred to as radio waves. Antennas are widely used in radio communication system. Which operate efficiently over a relatively narrow frequency band. An antenna must be tuned to the same frequency band as the radio system to which it is connected, otherwise

reception and/or transmission will be impaired. The electromagnetic behavior and the operation of antennas can be described by Maxwell's equations. Most antennas are resonant devices.

## 1.2 Types of Antenna

There are different types of antennas depending on their electrical characteristics, shape and size such as

<b>Wire Antennas</b>	<ul style="list-style-type: none"> <li>• Short Dipole Antenna</li> <li>• Dipole Antenna</li> <li>• Loop Antenna</li> <li>• Monopole Antenna</li> </ul>
<b>Log Periodic Antennas</b>	<ul style="list-style-type: none"> <li>• Bow Tie Antennas</li> <li>• Log-Periodic Antennas</li> <li>• Log-Periodic Dipole Array</li> </ul>
<b>Aperture Antennas</b>	<ul style="list-style-type: none"> <li>• Slot Antenna</li> <li>• Horn Antenna</li> </ul>
<b>Microstrip Antennas</b>	<ul style="list-style-type: none"> <li>• Rectangular Microstrip Patch Antenna</li> <li>• Quarter-Wave Patch Antenna</li> </ul>
<b>Reflector Antennas</b>	<ul style="list-style-type: none"> <li>• Flat-plate Reflector Antenna</li> <li>• Corner Reflector Antenna</li> <li>• Parabolic Reflector Antenna</li> </ul>
<b>Travelling-wave Antennas</b>	<ul style="list-style-type: none"> <li>• Long Wire Antenna</li> <li>• Yagi–Uda Antenna</li> <li>• Helical Wire Antenna</li> <li>• Spiral Antenna</li> </ul>
<b>Array Antennas</b>	<ul style="list-style-type: none"> <li>• Two-Element Array Antenna</li> <li>• Linear Array Antenna</li> <li>• Phased Array Antenna</li> </ul>

The regions surrounding the antenna are referred to as the “reactive near-field”, “radiating near-field” and “far-field”, or Fraunhofer region of an antenna.

### 1.3 Microstrip Patch Antenna

Microstrip patch antenna is mostly used in modern communication devices over conventional antennas mainly because of their size. Fig 1.2, shows the microstrip patch antenna. A patch antenna is a narrowband, wide beam antenna fabricated by etching the antenna element pattern in metal trace bonded to an insulating dielectric substrate such as a printed circuit board with a continuous metal layer bonded to the opposite side of the substrate which forms a ground plane. The EM waves is produced by an antenna which is so called transducer because it transforms electric current in to EM waves and by receiving vice versa.

Common microstrip antenna shapes are square, rectangular, circular and elliptical, but any continuous shape is possible. Microstrip antennas are best choice for wireless devices because of characteristics like low profile, low weight, ease of fabrication and low cost.

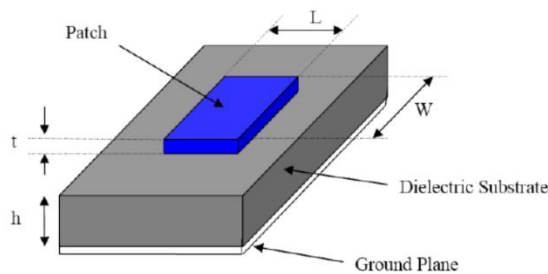


**Fig 1.2 Microstrip Patch Antenna**

The three essential parameters for the design of a rectangular Microstrip Patch Antenna:

- Frequency of operation ( $f_o$ ): The Mobile Communication Systems uses the frequency range from 2GHz to 6GHz. Hence the antenna designed must be able to operate in this frequency range. The resonant frequency selected for my design is 2.45 GHz.
- Dielectric constant of the substrate ( $\epsilon_r$ ): The dielectric material selected for our design is FR-4 which has a dielectric constant of 4.4.
- Height of dielectric substrate (h): For the microstrip patch antenna to be used in cellular phones. Hence, the height of the dielectric substrate is selected as 2.4mm.

A patch antenna is a type of radio antenna with a low profile, which can be mounted on a flat surface. It consists of a flat rectangular sheet or "patch" of metal, mounted over a sheet of metal called a ground plane. The assembly is usually contained inside a plastic radome, which protects the antenna structure from damage. The two metal sheets together form a resonant piece of microstrip transmission line with a length of approximately one-half wavelength of the radio waves. The radiation mechanism arises from discontinuities at each truncated edge of the microstrip transmission line. A patch antenna is usually constructed on a dielectric substrate, using the same materials and lithography processes used to make printed circuit boards. In general, microstrip antenna has a drawback of low bandwidth and low gain. The bandwidth can be increased by cutting slots and stacking configuration and Gain can be increased by using different patch elements in an array to achieve maximum radiation characteristics.

### **1.3.1 Advantages**

- Conformable to planar and non planar surfaces.
- Simple and inexpensive to manufacture using modern printed-circuit technology.
- Supports both, linear as well as circular polarization.
- Capable of dual and triple frequency operations.
- Mechanically robust when mounted on rigid surfaces, compatible with MMIC designs.

### **1.3.2 Applications**

- Used in high-performance aircraft,
- Spacecraft,
- Satellite, and missile applications,
- Mobile radio and wireless communication

## 1.4 Feeding Techniques

There are many configurations that can be used to feed microstrip antennas. Among them, four most popularly used feeding techniques are

- Microstrip line feed
- Coaxial probe feed
- Aperture coupling feed
- Proximity coupling feed

### 1.4.1 Microstrip line feed

The microstrip feed line is also a conducting strip, usually of much smaller width compared to the patch. The microstrip line feed is easy to fabricate, simple to match by controlling the inset position and rather simple to model. However as the substrate thickness increases, surface waves and spurious feed radiation increase, which for practical designs limit the bandwidth (typically 2–5%).

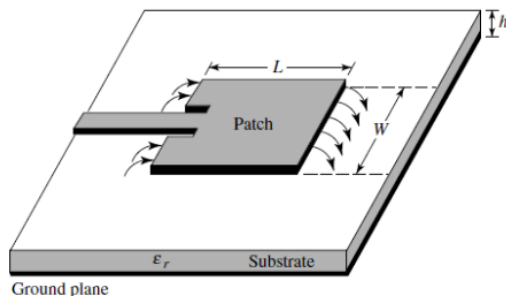
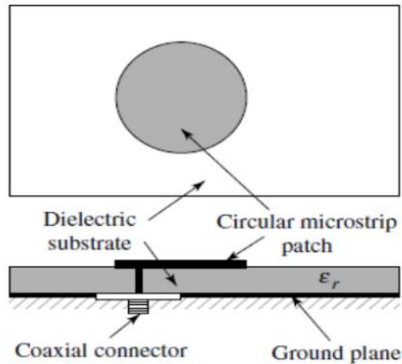


Fig 1.3Microstrip line feed

### 1.4.2 Coaxial probe feed

Coaxial feed or probe feed is a very common technique used for feeding microstrip patch antennas. Coaxial-line feeds, where the inner conductor of the coax is attached to the radiating patch while the outer conductor is connected to the ground plane, are also widely used. The coaxial probe feed is also easy to fabricate and match, and it has low spurious radiation. The main advantage of this type of feeding scheme is that the feed can be placed at any desired location inside the patch in order to match with its input impedance. However, it also has narrow bandwidth and it is more difficult to model, especially for thick substrates ( $h > 0.02\lambda_0$ ).



**Fig 1.4 Coaxial probe feed**

#### 1.4.2 Proximity coupled feed

Two dielectric substrates are used such that the feed line is between the two substrates and radiating patch is on top of the upper substrate. This type of feed technique is also called as “electromagnetic coupling scheme”. The proximity coupling has the largest bandwidth (as high as 13 percent), is easy to model and has low spurious radiation.

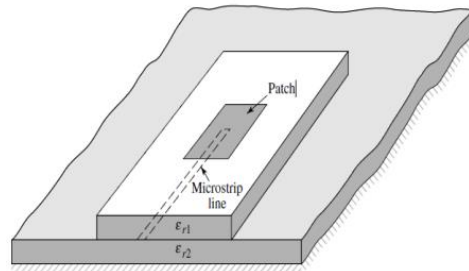


**Fig 1.5 Proximity coupled feed**

However its fabrication is more difficult. The length of the feeding stub and the width-to-line ratio of the patch can be used to control the matching.

#### 1.4.3 Aperture coupled feed

Both the microstrip feed line and the probe possesses inherent asymmetries which generate higher order modes which produce cross-polarized radiation. To overcome some of these problems, non-contacting aperture-coupling feeds have been introduced. The aperture coupling is the most difficult of all four to fabricate

and it also has narrow bandwidth. However, it is somewhat easier to model and has moderate spurious radiation. The aperture coupling consists of two substrates separated by a ground plane. Typically a high dielectric material is used for the bottom substrate, and thick low dielectric constant material for the top substrate. The ground plane between the substrates also isolates the feed from the radiating element and minimizes interference of spurious radiation for pattern formation and polarization purity.

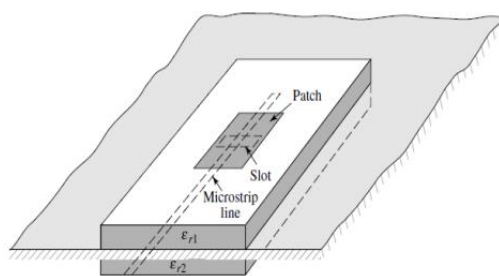


**Fig 1.6 Aperture coupled feed**

## 1.5 MIMO Antenna

Multiple Input Multiple Output (MIMO) have become popular in the recent years as they have shown improved results on spectral efficiency and capacity than the single antenna systems. MIMO plays a phenomenal role in the field of wireless communications by employing antennas with multiple elements at both sides of the communication link. It is a well known fact that the mutual coupling significantly affects their system performance.

MIMO Antenna systems including the antenna parameters like channel capacity, envelope correlation coefficient, total active reflection coefficient and total radiation efficiency are calculated .The MIMO antenna also exhibits an acceptable average peak gain.The mutual coupling changes the antenna characteristics in an array, and therefore, degrades the system performance of the MIMO system and causes the spectral re growth.

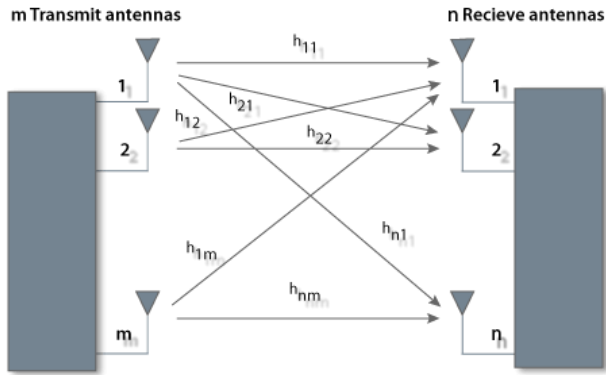


**Fig 1.7 MIMO**

## 1.6 Mutual Coupling

Mutual Coupling describes the energy absorbed by a nearby antenna when one antenna is operating. The mutual coupling tends to alter the input impedance, reflection coefficients, and radiation patterns of the arrayelements.

Mutual coupling is an electromagnetic phenomenon which exists in many antenna arrays. In most of the usual cases it is detrimental to the antenna operation. The mutual coupling between the two antenna elements in a MIMO system is related to the current direction that flows on the surface of the antennas. If the current flows in the same direction on the adjacent sides of both the antennas, the mutual coupling increases.

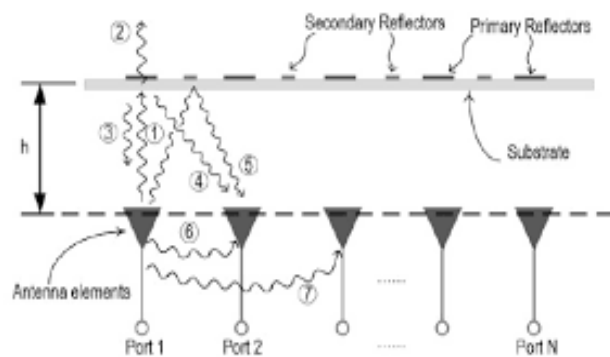


**Fig 1.8 Mutual coupling**

Mutual coupling (MC) can be quantified by measuring the antenna isolation. In addition, the antenna efficiency can be measured with and without the second antenna present; this will determine the magnitude of the efficiency loss due to the mutual coupling. MC between antennas will result in low antenna efficiency, poor impedance matching, and radiation performance. Thus, reducing MC involves various types of antennas, such as 3D non planar antenna array, waveguide slot array and microstrip patch antenna.

MC refers to the electromagnetic interactions between the elements of an antenna array. The effect of mutual coupling is that the electric field generated by one element alters the current distribution, as well as distorts the radiation/reception pattern of the other elements as compared to their isolated radiation/reception patterns. Moreover, the MC among array antennas depends on their radiation characteristics, relative separation and orientation.

### **1.7 Dual Layer Mushroom Structure**

IDLM is used to prevent the electromagnetic wave transmitting to the non-excitation element. IDLM unit consist of a double layer split-ring resonator. To reduce the surface current flow and the MC between the array radiating elements an array of IDLM have been implemented between the radiating elements. IDLM element is improved on the basis of double-layer rectangular EBG, which has a smaller size than simple double-layer EBG.

This structure can reduce the size of multi-element microstrip patch antennas (MPAs) by 61%. While the mushroom inner layer aids in the antenna miniaturization, the more compact upper layer acts as a band-stop filter further reducing the mutual coupling between the miniaturized patch antenna elements, which is otherwise not possible for a single-layer EBG structure. These periodic structures can suppress surface-waves in certain frequency bands called ‘stop-bands’ and subsequently reduce the MC between planar type antennas. The

uniplanar EBG structure was introduced in the super-substrate layer which reduced the mutual coupling by 10dB for an inter-element distance of  $0.5\lambda$  at 5.75GHz. Enhancements to the conventional mushroom structure are essential for designing compact MIMO systems.

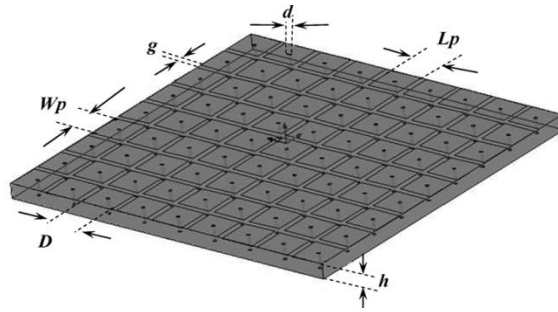


**Fig 1.9 EBG Structure**

### 1.8 E-Shaped Stub

To reduce the surface current flow and the MC between the array radiating elements, back-to-back E-shaped stubs have been implemented between the radiating elements. E-shaped stub can resonate at 2.45 GHz which is the center frequency of the antenna, so it can effectively prevent the electromagnetic wave from coupling to the adjacent antenna elements. The current is concentrated on the E-Shaped Stubs, the cross-polarization level of the antenna is almost unaffected.

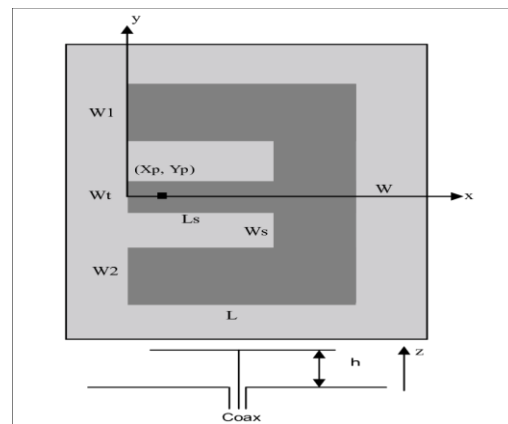


**Fig. 1.10: E-shaped stub**

E-shaped stub network is designed to create a reference electromagnetic wave to cancel the coupled waves. Slots can be in the form of S, U, L, E or H. But the E shape gives more enhanced bandwidth than other shape. Centre arm of E shape is like a tuning capacitor so widening the centre arm capacitance increases but the resonant frequency will be reduced.

### **1.9 Advantages**

- Simple feed can provide easy linear and circular polarization
- Maintains the radiation pattern characteristics of the phased array
- Minimize the effects of mutual coupling in a microstrip.
- The envelope correlation coefficient (ECC) of the designed antenna is low.
- The diversity gain (DG) is high ,very close to 10 dB.
- The total active reflection coefficient (TARC) is -11 dB at 2.45 GHz, which is available for MIMO system.
- The use of DGS can suppress the surface wave and improve isolation.
- The proposed decoupling structure can also improve the average gain and efficiency of the antenna by 0.1 dB and 5%, respectively.
- Structure resembles a good antenna performance of small size.
- Produced better impedance bandwidths

### **1.10 Applications**

- Wireless system communication
- Radio technology
- Satellite communication
- Mobile communication
- Environmental instrumentation and remote sensing.
- Biomedical radiator communications.
- Aircraft and missiles.

## CHAPTER 2

### LITERATURE REVIEW

#### **(1) “ISOLATION IMPROVEMENT OF MIMO ANTENNA USING A NOVEL FLOWER SHAPED METAMATERIAL ABSORBER AT 5.5GHz WiMAX BAND” was designed by PriyankaGargandPriyanka Jainin 2021.**

In this paper the use of metamaterial absorber (MA) to achieve high isolation between two patch antennas in a 2-element MIMO system operating at 5.5 GHz resonant frequency useful for WiMAX application is proposed. The proposed flower shaped MA, designed on a  $9 \times 9\text{mm}^2$  FR-4 substrate with 1 mm thickness, exhibits near unity normalized impedance at 5.5 GHz with an absorptivity of 98.7 %. A 4-element array of the MA is arranged in the form of a line in the middle of the two radiating patches in order to suppress the propagation of surface current between them at the operating frequency. Using the proposed flower shaped MA, an isolation of nearly 35 dB is achieved. The MIMO structure is studied in terms of return loss, isolation, overall gain, radiation pattern, Envelope Correlation Coefficient (ECC), Diversity Gain (DG), and Total Active Reflection Coefficient (TARC) etc. The structure is finally fabricated and measured to show good agreement with the simulated results. Use of MIMO (multiple-input-multiple output) antennas has increased in modern wireless communication systems as they offer significant improvement in link range as well as data throughput within the available bandwidth and power. Due to increased demand of miniaturization, mutual coupling reduction in MIMO antenna systems is the major issue of concern. Various techniques are available in literature to overcome this problem. Metamaterials are the artificial structures that are being extensively used to improve the characteristics of various microwave components. In this paper, the use of metamaterial-based absorber for mutual coupling reduction in MIMO antenna has been explored. Such devices can start to resonate over a certain frequency range when an electromagnetic wave is incident upon them achieving near unity or so-

called “perfect absorption”. Such metamaterial absorbers are being utilized for several applications such as radar cross section (RCS) reduction, energy harvesting, sensing and so on.

**(2) “NOVEL AND EFFICIENT PARASITIC DECOUPLING NETWORK FOR CLOSELY COUPLED ANTENNAS”** was designed by **Min Li, Lijun Jiang and Kwan Lawrence Yeung** in **2019**.

A novel and efficient parasitic decoupling network (PDN) is proposed for closely coupled antennas. In this paper, it provides a new perspective and approach to design decoupling networks based on the parasitic decoupling concept. The PDN is composed of sections of transmission lines (TLs) and reactive components, allowing additional power-traveling paths. With the TL lengths and reactive component reactance's being precisely determined, the traveling power from one antenna to another could cancel out the undesired power wave induced by mutual coupling, resulting in the high port isolation. The decoupling theory is rigorously derived with the design procedure of the PDN systematically described in connection with two examples of the two- and three-element monopole arrays. The measurement results show that good impedance matching for each antenna port, isolations of more than 25 dB, total efficiencies of more than 64%, and envelop correlation coefficients (ECCs) of less than 0.07 are attained simultaneously for both examples using the proposed PDN. The results verified the decoupling theory and proved the PDN concept.

**(3) “ISOLATION ENHANCEMENT IN DUAL-BAND MICROSTRIP ANTENNA ARRAY USING ASYMMETRIC LOOP RESONATOR”** was designed by **Lakshmi Devi, Kuttathati Srinivasan Vishvaksenan and Kalidas Rajakani** in **2018**

The design of a wideband decoupling element for mutual coupling reduction in microstrip antenna arrays is demonstrated. The proposed decoupling unit cell

consists of an asymmetric loop resonator with a coupled microstrip line for wide stop-band characteristics from 2 – 5 GHz. The band gap characteristic of the decoupling element is analyzed, and the results are presented. Further the resonator is deployed in a two-element dual band microstrip antenna array and mutual coupling reduction is demonstrated. The decoupling unit cell has a lateral dimension of 2.84 mm and hence enables the packing of antenna elements in very close proximity with reduced mutual coupling. The proposed solution offers additional isolation greater than 15 dB in a V-slot loaded dual-band antenna with edge-to-edge element spacing of  $0.057\lambda_0$ . The prototype dual-band antenna array with decoupling element is fabricated and the simulation results are validated using experimental measurements.

**(4) “REDUCTION OF MUTUAL COUPLING BETWEEN PATCH ANTENNAS USING POLARIZATION-CONVERSION ISOLATOR” was designed by You-Feng Cheng, Xiao Ding, Wei Shao, and Bing-Zhong Wang in 2017**

A novel approach to suppress mutual coupling (MC) between two patch antennas is presented in this paper. A parasitic isolator, which is printed between the two patches, controls the polarization of the coupling field to reduce the antenna coupling. Furthermore, a defected ground structure (DGS) is employed to suppress the cross-polarization (XP) level. There exists a trade-off between the MC reduction and XP improvement in this approach. As an example, a two-element patch array with an optimized isolator is fabricated and measured. The measured results show that, at the resonant frequency, the achieved isolation enhancement and XP level are 19.6 dB and -13.2 dB, respectively. In, a simple U-shaped microstrip was utilized to create an indirect signal coming via the extra coupling path that opposes the signal going directly from the active element. In, an asymmetrical coplanar strip, inserted vertically between two antennas, was adopted to generate.

**(5) “VERY COMPACT FULLY LUMPED DECOUPLING NETWORK FOR A COUPLED TWO-ELEMENT ARRAY” was designed by Cheng-Hsun Wu, Chia-Lin Chiu and Tzyh-Ghuang Ma in 2016**

Without the need of any transmission line, a very compact decoupling network based on reactive lumped elements is presented for a two-element closely spaced array. The lumped network consisting of two series and four shunt elements can be analytically designed using the even–odd mode analysis. In the even mode, the half-circuit of the decoupling network is identical to an L-section matching network, while in the odd mode it is equivalent. The proposed decoupling network can deal with the matching conditions of the even and odd modes independently to simultaneously achieve good impedance matching and port isolation of the whole antenna array. The design principle, formulation, and experimental results including the radiation characteristics are introduced.

**(6) “An Efficient Decoupling Feeding Network for Microstrip Antenna Array” was designed by Run-Liang Xia, Shi-Wei Qu, Peng-Fa Li, Qi Jiang and Zai-Ping Niein 2015**

In this paper, an efficient decoupling feeding network is proposed. It is composed of two directional couplers and two sections of sections of transmission line connection use. By connecting the two couplers, an indirect coupling with controlled magnitude and phase is introduced, which can be used to cancel out the direct coupling caused by space waves and surfaces waves between array elements. To demonstrate the method, a two-element microstrip antenna array with the proposed network has been designed, fabricated and measured. Both simulated and measured results have simultaneously proved that the proposed method presents excellent decoupling performance. The measured mutual coupling can be reduced to below -58 dB at center frequency. Meanwhile it has little influence on return loss and radiation patterns. The decoupling mechanism is simple and straightforward which can be easily applied in phased array antennas and MIMO systems.

**(7) “DUAL-LAYER EBG-BASED MINIATURIZED MULTI-ELEMENT ANTENNA FOR MIMO SYSTEMS” was designed by Soham Ghosh, Thanh-Nguyen Tran, and Tho Le-Ngoc in 2014**

A dual-layer electromagnetic bandgap (EBG) mushroom structure is proposed in this paper. Based on the concept of slow-wave propagation, this structure can reduce the size of multi-element microstrip patch antennas (MPAs) by 61%. While the mushroom inner layer aids in the antenna miniaturization, the more compact upper layer acts as a band stop filter further reducing the mutual coupling between the miniaturized patch antenna elements, which is otherwise not possible for a single-layer EBG structure. Various 2- and 4- element miniaturized MPAs are proposed for 2.5GHz band applications, with antenna elements closely spaced at  $0.5\lambda$  and low mutual coupling levels in the range of -28dB to -50dB. Furthermore, the achievable multiple-input-multiple-output (MIMO) channel capacities of these miniaturized multi-antennas are analysed using the Kronecker channel model and tested in various propagation scenarios like the anechoic chamber, reverberation chamber and indoor. It is observed that the miniaturized MPAs can provide significant gains in MIMO capacity in all the signal scattering environments.

**(8) “REDUCING MUTUAL COUPLING OF CLOSELY SPACED MICROSTRIP MIMO ANTENNAS FOR WLAN APPLICATION” was designed by J.Ou Yang, F.Yang, Z. M. Wang in 2014**

An efficient mutual coupling reduction method is introduced in this letter for extremely closely placed dual element microstrip antennas positioned on a finite-sized ground plane for WLAN MIMO application at 5.8 GHz. High isolation can be achieved through a simple slot structure on the ground between the microstrip antennas. The position, length, and width of the slot have been optimized for maximizing the isolation. It is found that more than 40 dB isolation can be achieved between two parallel microstrip antennas sharing a common ground plane. The space distance of these antenna is 17.5mm 0.33 from element Centre to Centre (side

by side of 1.6mm 0.33) when the ground plane size is 0.85x 0.55. Along with this letter, several prototypes were fabricated, and their performances measured to validate the obtained IE3D moment method-based simulation results. The mutual coupling or isolation between closely placed antenna elements is important in a number of applications. These include systems relying on array antennas and more recently multiple-input–multiple-output (MIMO) wireless communication systems. The best isolation values are always found when the antennas are spaced by the largest available distance on the PCB. In, single-negative magnetic (MNG) metamaterials were developed in order to efficiently suppress the electromagnetic coupling between closely spaced antenna elements. Another mechanism proposed previously was to decorrelate the isolate highly coupled monopole antenna elements by using highly couplers. In a resonator between the antennas was introduced to reduce the mutual coupling. In, linking the two planar inverted-F antennas (PIFAs) by a suspended microstrip line or the link of both shorting strips of the PIFAs were used to decrease the mutual coupling between two PIFAs respectively radiating in the DCS 1800 and UMTS bands.

**(9) “MUTUAL COUPLING REDUCTION BETWEEN MICROSTRIP PATCH ANTENNAS USING SLOTTED-COMPLEMENTARY SPLIT-RING RESONATORS”** was designed by **Mohammed M. Bait-Suwailam, Omar F, Siddiqui, and Omar M. Ramhiin 2010**

A novel structure based on complementary split-ring resonators (SRRs) is introduced to reduce the mutual coupling between two coplanar microstrip antennas that radiate in the same frequency band. The new unit cell consists of two complementary SRR inclusions connected by an additional slot. This modification improves the rejection response in terms of bandwidth and suppression. The filtering characteristics of the band-gap structure are investigated using dispersion analysis. Using the new structure, it was possible to achieve a 10-dB reduction in the mutual coupling between two patch antennas with a separation of only 1/4 free-

space wavelength between them. Since the proposed structures are broadband, they can be used to minimize coupling and co-channel interference in multiband antenna. Surface waves and near fields can lead to coupling between coplanar and patch antennas. The near field coupling arises when an antenna is placed in the near-field zone of another antenna. The near-field coupling is strong in situations where the antennas are printed on dielectric substrates with very low permittivity. In such scenarios, the coupling can result in severe degradation to the antenna's radiation characteristics. While surface waves are weakly excited in very thin grounded dielectric substrates, space-waves dominate and show strong coupling when antennas are in proximity. In electromagnetic bandgap (EBG) structures using the mushroom-like topology were used. However, the structures involved plated through-holes (vias), which are not attractive from the electric loss and manufacturing perspective.

## CHAPTER 3

### ANTENNA DESIGN AND ANALYSIS

#### 3.1 OVERVIEW

In multiantenna applications such as MIMO system, Rx/Tx system, and array antenna, the coupling between neighboring antenna elements is an important problem that cannot be ignored. The MC between antennas will result in low efficiency, poor impedance matching and radiation performance. Thus, reducing MC involves various types of antennas, such as 3D non-planar antenna array, waveguide slot array and microstrip patch antenna .As one of the most commonly used antennas, microstrip antenna is extensively employed in many wireless system. The extent of this project is to designthe improved IDLM and back-to-back E-shaped stubs for mutual coupling reduction between microstrip patch antennas are presented in this paper. The IDLM unit consists of one upper layer split-ring resonator lattice and four lower layer lattices. The decoupling structure can prevent the surface current from one antenna port to another, so as to improve the isolation between the antennas. The proposed antenna works in the open wireless communication band of 2.45 GHz. A low mutual coupling level ranging from  $-27$  to  $-40$  dB is obtained when the center distance of the adjacent patches is  $0.5\lambda_0$ . The total size of the decoupling antenna is  $99 \times 41 \times 2.4\text{mm}^3$  with a frequency range of 2.42–2.48GHz for  $S_{11}<-10\text{dB}$ . The proposed decoupling structure can also improve the average gain and efficiency of the antenna by 0.1 dB and 5%, respectively. The antenna is studied from the aspects of isolation, return loss, current and electric field distribution, radiation pattern, and diversity performance. The designed decoupling antenna is fabricated and measured. The pattern, isolation, and return loss of the tested results show good consistence with the simulation results. The diversity gain and envelop correlation coefficient of the diversity performance show that the designed antenna can be used in MIMO or Rx/Tx systems.

### 3.2 Structure of Antenna.

The structure and geometry of the designed antenna are provided in Fig 3.2(a). The substrate of the antenna is FR4 with loss tangent ( $\delta$ ) of 0.02, and the total size of the antenna is  $99 \times 41 \times 2.4\text{mm}^3$ . It consists of four IDLM elements and two back-to-back E-shaped stubs, which are located between the two antenna elements.

The resonant frequency of the designed antenna is about 2.45GHz. To obtain this resonance frequency, the patch antenna dimensions are as follows:  $L_p = 24.4\text{mm}$  and  $W_p = 27.4\text{ mm}$ . The two antenna elements are fed by a coaxial probe is shown in Fig. 3.1, respectively. The center-to-center spacing (S1) of the element is 64.1mm, which is equivalent to half of the wavelength corresponding to 2.45GHz.

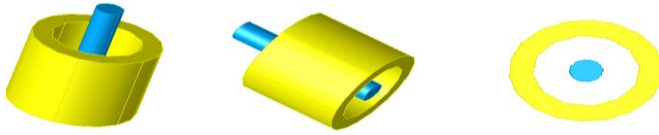


**Fig 3.1 Coaxial probe**

To reduce the surface current flow and the MC between the array radiating elements, back-to-back E-shaped stubs and an array of IDLM have been implemented between the radiating elements. The IDLM units consist of a double-layer split-ring resonator with a similar structure shown in Fig 3.2(b). The lower layer consists of four elements of the same size, and the upper layer is an element of another size. The resistance band of the IDLM is used to prevent the electromagnetic wave transmitting to the nonexcitation element. The specific parameters of the optimized IDLM are shown in Table 1

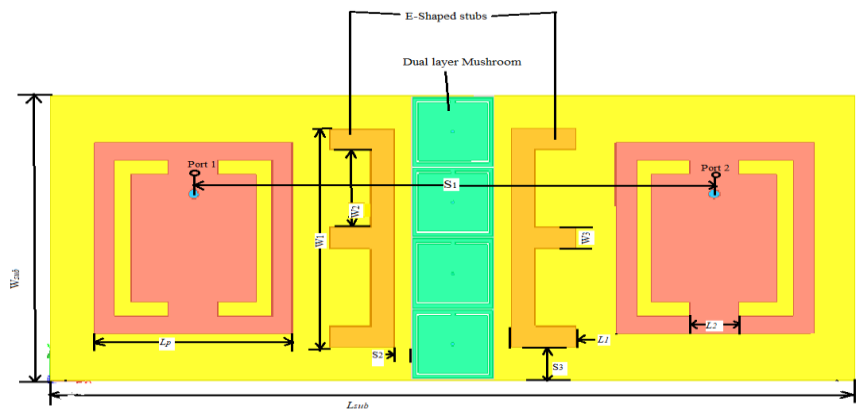


**Fig 2(a) Geometry of the proposed antenna**

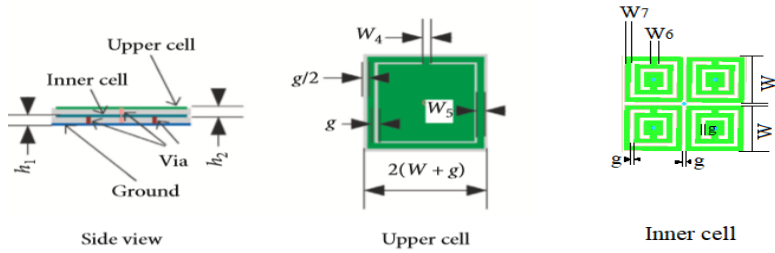


**Fig 2(b) dual-layer mushroom**

The length of  $L_1 + W_1/2 - W_3$  in the E-shaped stub is about one-fourth of the effective wavelength corresponding to 2.45GHz. The E-shaped stub can resonate at 2.45GHz which is the center frequency of the antenna, so it can effectively prevent the electromagnetic wave from coupling to the adjacent antenna element. The relationship between the length of E-shaped stubs and S21 of the adjacent antenna elements.  $W_1$  remains unchanged at 27.4mm when  $L_1$  changed, and  $L_1$  remains unchanged at 8mm when  $W_1$  changed .It can be seen that, with the increase in  $L_1$  or  $W_1$ , the frequency with a smaller S21 value gradually decreases because the increase in  $L_1$  or  $W_1$  leads to the decrease in the resonance frequency. By adjusting  $L_1$  or  $W_1$ , the isolation of the required frequency band can be improved. The optimized parameters of the E-shaped stubs are shown in Table 1.

Parameters	Dimension (mm)
$W_1$	31.4
$W_2$	11.2
$W_3$	3
$L_1$	8
$L_2$	6.1
$W$	4.8
$g$	0.3
$h_1$	1.2
$h_2$	1.2
$W_4$	0.6
$W_5$	0.5
$W_6$	0.6
$W_7$	0.5

**Table 1 Dimensions of optimized parameters of the proposed system**

Next, the position of the E-shaped stub is explored. The S-parameter results variation for various spacing (S2) between the E-shaped stub and IDLM. S3 remains unchanged at 7.2mm, and the other parameters of the antenna are listed in Table1 when S2 changed. As S2 increases from 1 to 3mm and then 6mm, the S21 decreases from  $-23.7\sim-27.4$  to  $-24.9\sim-36.2$ dB and then increases to  $-24.5\sim-35.1$ dB. The resonate frequency of the antenna increases with the increase in S2. The best S-parameter is obtained when S2=2.15mm. The effect of E-shaped stub on set (S3) on the decoupling performance. S2 remains unchanged at 2.15mm, and the other parameters areas Table 1 when S3 changed. When S3=4.8mm, that is the E-shaped stub on sets too far from the center of the radiation patch, the frequency of S21 minimum becomes higher. This is because the effective length of the E-shaped stub becomes smaller. However, when S3 increases to 4.8mm, the S21 remains almost unchanged in the operating frequency band of the antenna.

Illustrates the S-parameter results versus frequency for the various center-to-center spacing (S1). As S1 reduces from 64.1mm to 56.1mm, the isolation is less affected, while the frequency corresponding to the minimum value of S11 increases.

### **3.3 Coupling Reduction Performance.**

The configurations of the three antennas are presented in Fig.3.3: (1)AT1 is a dual conventional rectangular antenna without decoupling structure, (2) AT2 is a dual antenna with an array of IDLM, and (3) AT3 is a dual antenna with back-to-back E-shaped stubs on both sides of the IDLM.

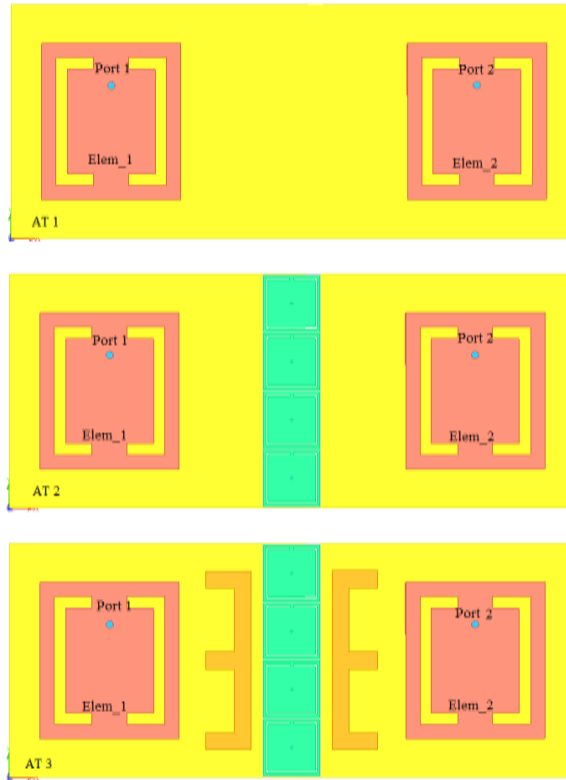


**Fig 3.3 Configuration of Ant 1, Ant 2, and Ant 3**

The transmission coefficient ( $S_{21}$ ) and simulated reflection coefficient ( $S_{11}$ ) of the abovementioned three antennas. It is observed that AT1 has poor isolation. The MC of AT2 is slightly lower than that of AT1 because there are fewer IDLM elements in a limited space. The MC of AT3 is obviously improved by printing E-shaped stubs on both sides of the IDLM. The minimum coupling degree is reduced by approximately 20dB, which is less than  $-27\text{dB}$  in the entire working bandwidth.

To express the reason for the increased isolation, the surface current distribution of AT1, AT2 and AT3 at 2.45 GHz. In the analysis, port 1 is excited and port2 is loaded with a  $50 \Omega$  standard resistance. Before loading decoupling structure, the current induced by the right element is high when the left unit is excited. Therefore, the MC between elements of AT1 is high. The MC is reduced when IDLM is employed. The current on the right element decreases, but a part of current is still coupled to the right element. When introducing E-shaped stubs on

both sides of the IDLM, most of the current is concentrated on the E-shaped stubs, resulting in a small-induced current on the right element. Therefore, the isolation is greatly improved.

To further analyze the influence of decoupling structure on antenna performance, the electric field without or with the decoupling structure is shown in Figure 3.4. The electric field of excitation element is almost unaffected by the decoupling structure. But the electric field of non-excited element rotates about 45 degrees. Therefore, the far-field pattern radiated by the right element has almost no effect on the copolarization pattern of the excited element. That is why the copolarization pattern of the excited element is not affected by the nonexcited element with the decoupling structure introduced. It can also be seen from the figure that, with introducing the decoupling structure, the feed point of the nonexcited element is at the minimum position of the electric field, so the feed port isolation between the two elements is improved.

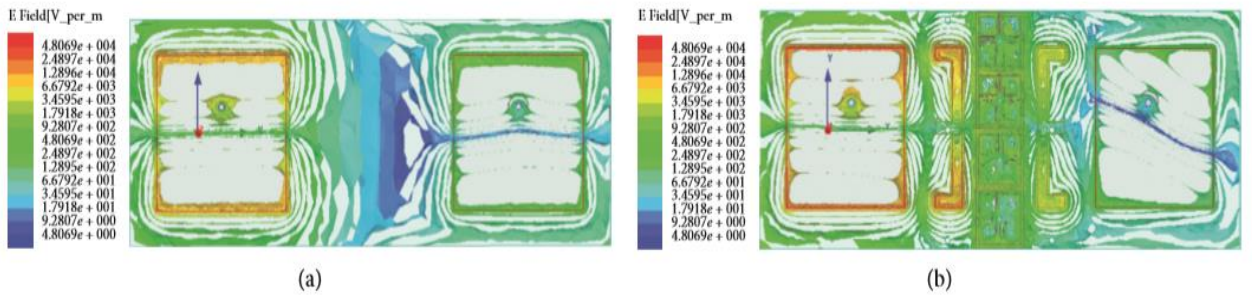


**Fig 3.4 Electric field distribution: (a) AT1;(b) AT3**

The proposed decoupling structure in this paper is also effective for PIFAs. The S-parameters of 2-element PIFAs with and without the proposed decoupling structure is compared when the center distance of the PIFAs remains  $0.5\lambda_0$ . It is observed that the minimum coupling value is reduced by approximately 10dB, which is less than – 35dB in the entire working bandwidth.

### 3.3 Substrate material

The design of coupler will starts with specifying the proper substrate. Table 2 shows the specification of Flame-Retardant 4 (FR-4), the chosen laminate in this work. FR-4 is preferred over cheaper alternatives.

It is lossy at high frequencies, absorbs less moisture, has greater strength and stiffness and is highly flame resistant compared to its less costly counterpart.

FR-4 is widely used to build high-end consumer, industrial and military electronic equipment.

FR-4 is a composite material composed of woven fiber glass cloth with an epoxy resin binder that is flame resistant (self-extinguishing). FR4 is a grade designation assigned to glass-reinforced epoxy laminate sheets, tube, rods and printed circuit boards (PCB).

FR-4 epoxy resin systems typically bromine, a halogen, to facilitate flame-resistant properties in FR-4 glass epoxy laminates. Some application where thermal destruction of the material is a desirable trait will still use G-10 non flame resistant.

PARAMETERS	VALUE
Dielectric constant	4.4
Substrate	FR4
Loss tangent ( $\delta$ )	0.02
Thickness	2.4mm
$Z_0$	50Ω

**Table 2 FR-4 Specification**

### **3.5 Application of Antenna**

- Wireless system communication.
- Radio Technology.
- Satellite Communication.
- Mobile Communication.
- Structure resembles a good antenna performance of small size.
- Produced better impedance bandwidths.

## CHAPTER 4

### RESULTS AND DISCUSSION

The proposed design was simulated using commercially available simulator. The simulator was used in Windows platform. The model designed here is a design of Mutual Coupling Reduction Using Improved Dual-Layer Mushroom and E-Shaped Stub

#### **4.1 ADS**

Advanced Design System (ADS) is an electronic design automation software system produced by Key sight EEs of EDA, a division of Key sight Technologies. It provides an integrated design environment to designers of RF electronic products such as mobile phones, pagers, wireless networks, satellite communications, radar systems, and high-speed data links. Key sight ADS supports every step of the design process schematic capture, layout, design rule checking, frequency-domain and time-domain circuit simulation, and electromagnetic field simulation this allow us to fully characterize and optimize an RF design without changing tools.

##### **4.1.1 Key features**

- Complete schematic capture and layout environment.
- Innovative and industry leading circuit and system simulators.
- Direct, native access to 3D planar and full 3D EM field solvers.
- Up-to-date Wireless Libraries enable design and verification of the latest emerging wireless standards.
- EM simulator operates on a physical layout description of the component/circuit.
- It is possible to interface the EM simulator with the drafting software which is used to draw the physical structure and mask layouts.
-

## 4.2 Design layout of proposed model

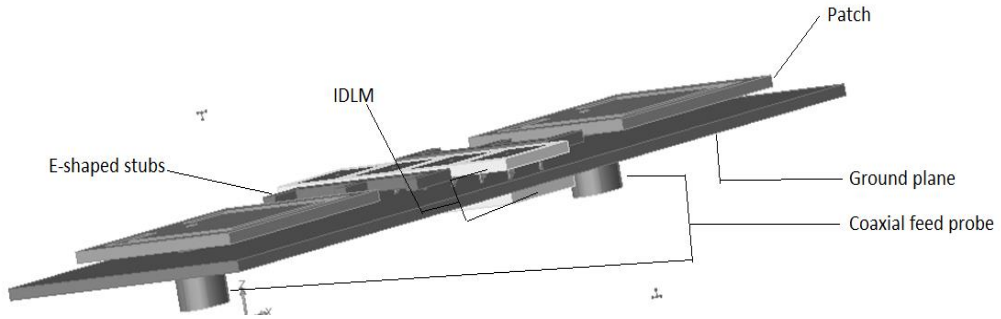


**Fig 4.1 Model of patch with feed**

## 4.3 Performance analysis

The performance of the proposed design is described with the help of following parameters

- Return loss
- Isolation
- Insertion loss
- Gain
- Axial ratio
- Radiation pattern

## 4.4 Experimental Result and Discussion

To validate the MC performance of the designed antenna, a prototype is fabricated and measured in an anechoic chamber. The S-parameters and radiation patterns are simulated and measured. The ECC, DG, and TARC are studied to further evaluate the diversity performance.

### 4.4.1 Antenna Performance.

The S-parameters of the designed antenna are simulated and measured, and the results are illustrated in Fig. 4.2. The measured result of S11 shows that the resonant frequency of the antenna is 2.45 GHz, which is 0.02 GHz lower than the

simulated result. The slight shift in the resonance frequency may be due to common factors, such as the tolerance on the FR4 dielectric constant, inaccuracy in the fabrication process, and effect of the SMA connector.

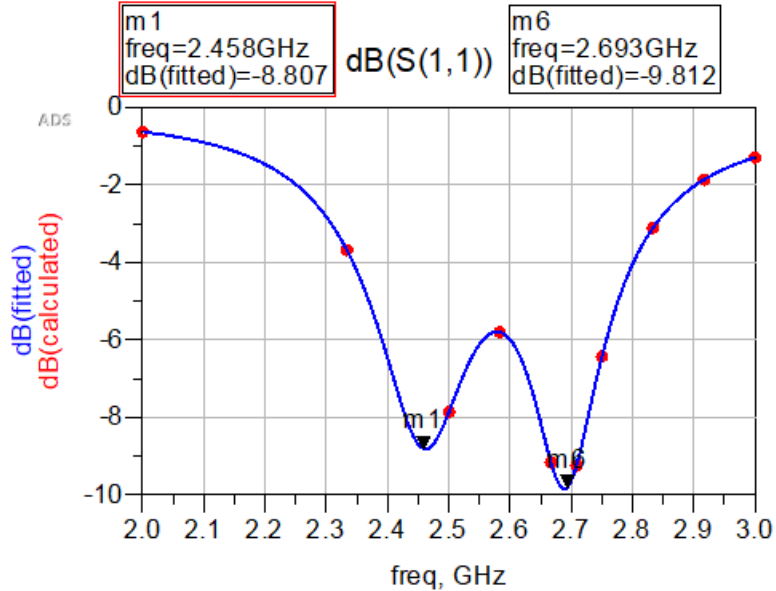


**Fig 4.2 Simulated and measured S-parameter**

The simulated S<sub>21</sub> of the operating frequency is  $-38.6$  dB, and the measured is  $-10$  dB. The MC of the proposed antenna is less than  $-10$  dB within the operation bandwidth of  $-10$  dB. Fig.4.3 shows the radiation patterns of measured and simulated when one port of the antenna is excited and the other port is connected to  $50\Omega$  resistance. The measured results correspond with the simulated results. In the main lobe patterns of the upper-sphere space, the simulation and measurement results are basically consistent. The proposed decoupling structure of increasing isolation can effectively reduce the influence of the adjacent element on the main lobe of the pattern. With the insertion of IDLM and E-shaped stub, the cross-polarization level of the antenna is almost unaffected. Within 3 dB beam width, the relative cross-polarization level is greater than 18dB.

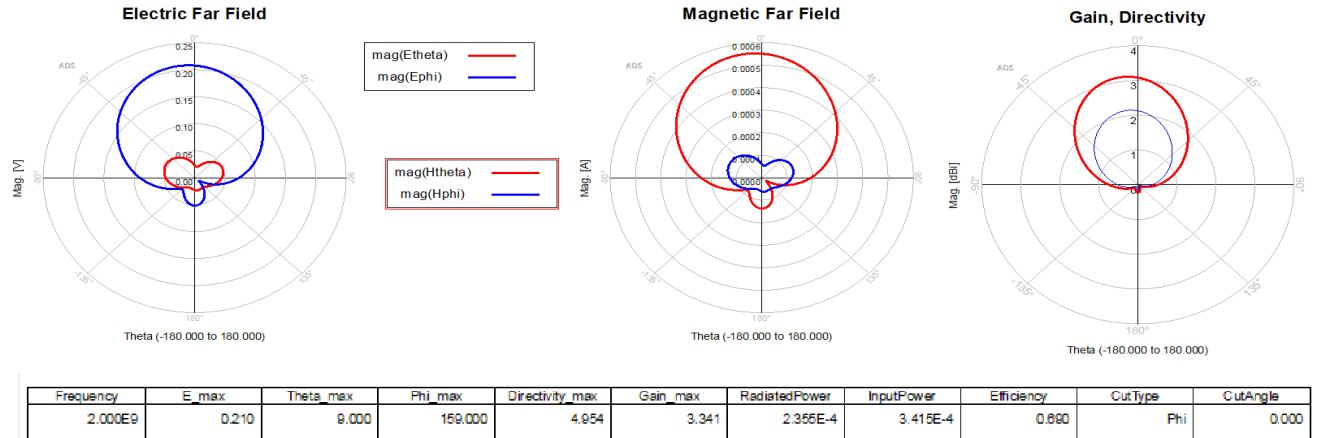


**Fig 4.3 Simulation and measured far-field**

The simulated and measured gain and radiation efficiency of the AT1 and AT3 are shown in Fig 4.4. It can be seen that the simulated efficiency of AT1 and AT3 are 47% and 51% at 2.45 GHz, respectively. When the frequency is higher than 2.45 GHz, the gain and efficiency of AT3 are improved because the matching and isolation of AT3 is better than that of AT1. The gain and efficiency of AT3 are basically consistent with the simulation results.

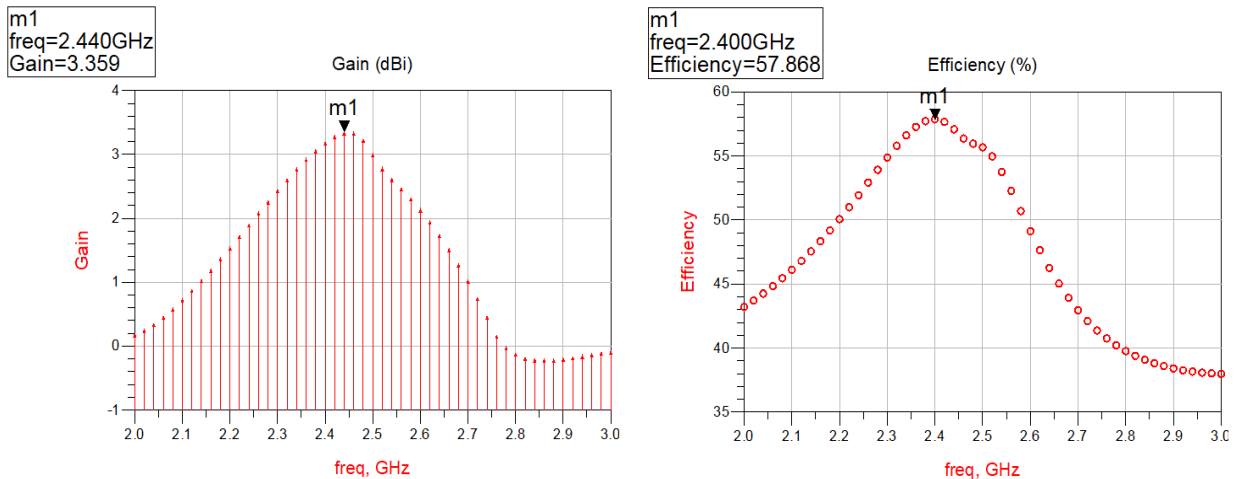


**Fig 4.4 Gain and Efficiency**

This method is compared with the common mutual coupling suppression methods of microstrip radiation patch, as shown in Table 2. It can be seen that the proposed method of combining the stub and EBG can achieve a better isolation than

others with the same center-to-center spacing. Although the antenna in achieves a wider bandwidth and better isolation, it has a higher profile and larger spacing.

Method	$f_0$ (GHz)	Freq. range	Max isolation	Center-to-	Total size (mm)
		( $ S_{11}  < 10$ dB)	(dB)	center spacing	
<b>EBG</b>	5.1	/	30	$0.5\lambda_0$	$>0.82 \lambda_0 \times 0.50 \lambda_0 \times 0.03 \lambda_0$
<b>EBG</b>	5	2.4%	34	$0.5\lambda_0$	$1.3 \lambda_0 \times 1.0 \lambda_0 \times 0.02 \lambda_0$
<b>Decoupling feeding network</b>	7.5	9.2%	58	$0.65\lambda_0$	$\lambda_0 \times 1.01 \lambda_0 \times 0.2 \lambda_0$
<b>Stub and EBG</b>	2.45	2.4	39	$0.5\lambda_0$	$0.81 \lambda_0 \times 0.33 \lambda_0 \times 0.02 \lambda_0$

**Table 3: Dimension of optimized parameters of the proposed antenna**

#### 4.4.2 Diversity Analysis.

To evaluate the diversity characteristic, the ECC and DG of the designed antenna are estimated. The ECC can be calculated using S-parameters or far-field vector phasor radiation patterns. In “Exact representation of antenna system diversity performance from input parameter description”, the author has verified that the two methods are equivalent in calculating the ECC of half-wave dipoles and orthogonal fed microstrip antennas. Comparing with a radiation pattern method, S-parameter method is more convenient in data acquisition and calculation. When the radiation efficiency of the antenna is low, the radiation efficiency should be considered while using S-parameter to calculate ECC as equation (1), where  $S_{aa}$  and  $S_{bb}$  represent the reflection coefficients of the two element ports,  $S_{ab}$  and  $S_{ba}$  represent the transmission coefficients of the two element ports, and  $\eta_a$  and  $\eta_b$  are the radiation efficiencies of the two elements:

$$\text{ECC} = \frac{|S_{aa}^* S_{ab} + S_{ba}^* S_{bb}|^2}{(1 - |S_{aa}|^2 - |S_{ba}|^2)(1 - |S_{bb}|^2 - |S_{ab}|^2)\eta_a\eta_b}. \quad (1)$$

The DG can be estimated by ECC, and the calculation formula is shown as follows:

$$DG = 10 \sqrt{1 - (ECC)^2}. \quad (2)$$

The ECC and DG of the proposed antenna are illustrated. The simulation results are in good agreement with the measured in the range of 2.42–2.48 GHz. The estimated value of ECC is far less than the commonly used threshold level of 0.5, and the value of DG is large, very close to 10dB. These characteristics show that the designed antenna has good diversity performance and is suitable for Rx/Tx or MIMO system.

Total active reflection coefficient (TARC) is another important parameter to evaluate the diversity performance. The TARC can be calculated by equation (3). When TARC is less than 0 dB, MIMO system can work normally. The simulated and measured TARC are – 6 dB and – 11 dB for the desired frequency 2.45 GHz:

$$TARC = \sqrt{\frac{|(S_{aa} + S_{ab})|^2 + |(S_{ba} + S_{bb})|^2}{2}}. \quad (3)$$

## 4.5 Simulated Result

### 4.5.1 Return loss

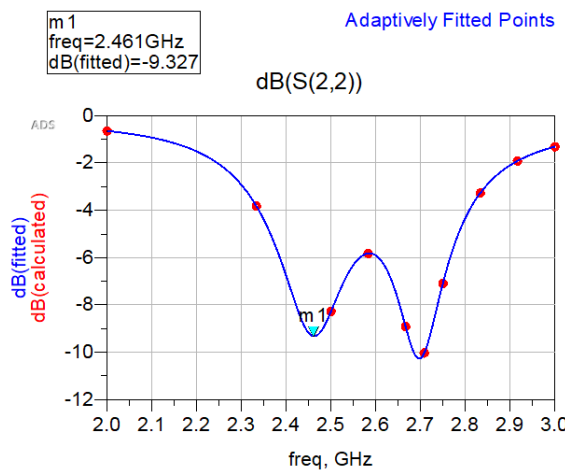


**Fig 4.5 Return loss**

The return loss is an another way of expressing mismatch. It is a logarithmic ratio measured in dB that compares that power reflected by the antenna to the power that is fed into the antenna from the transmission line. Fig. 4.5 shows the return loss.

#### 4.5.2 Isolation

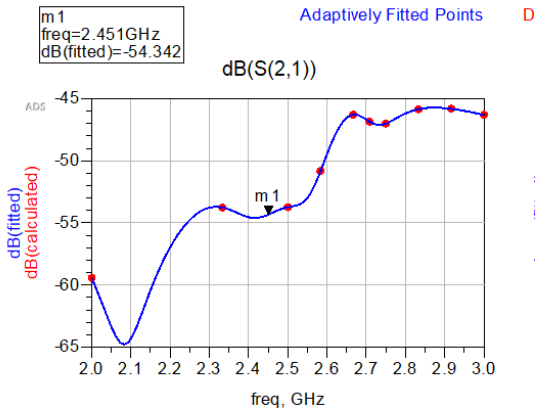


**Fig 4.6 Isolation loss measured**

In an ideal coupler the output ports are mutually isolated. In other words, a signal entering output 2 does not leak out of output 3. Isolation is defined as the ratio of a signal entering output 1 that is measured at output 2, assuming all ports are impedance matched. Fig.4.6 shows the isolation loss measurement.

#### 4.5.3 Insertion loss

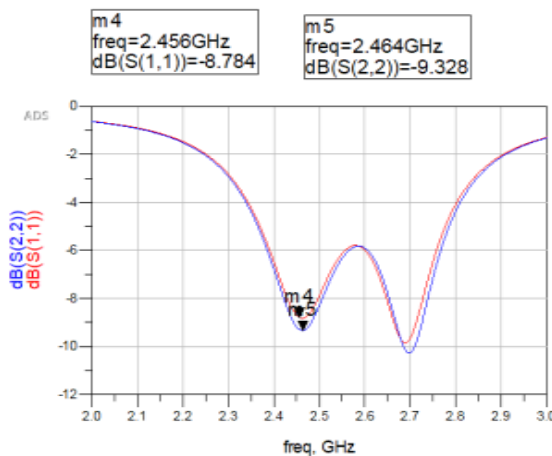


**Fig 4.7 Measurement of insertion loss in dB**

The above output (Fig 4.7) shows the insertion loss measurement of the proposed system in dB. The marking (m4,m5) shows the reading of the insertion loss

#### 4.5.4 Gain

Gain of an antenna in a given direction is defined as —the ratio of the intensity, in a given direction, to the radiation intensity that would be obtained if the power accepted by the antenna were radiated isotropically.

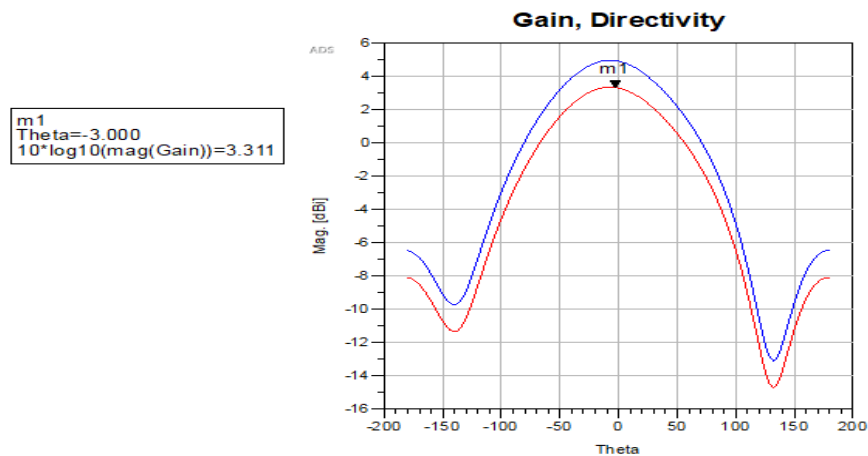


**Fig 4.8 Gain pattern of proposed model**

#### 4.5.5 Axial ratio

The axial ratio is the ratio of orthogonal components of an E-field. Axial ratios are often quoted for antennas in which the desired polarization is circular. The ideal value of the axial ratio for circularly polarized fields is 0 dB. In addition, the axial ratio tends to degrade away from the main beam of an antenna, so it indicates that the deviation from circular polarization is less than 3 dB over the specified angular range. Fig. 4.9: shows axial ratio as 8.633

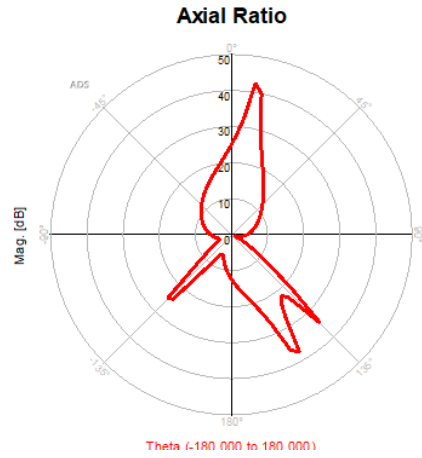


**Fig 4.9 Axial Ratio of the proposed model**

#### 4.5.6 Radiation Pattern

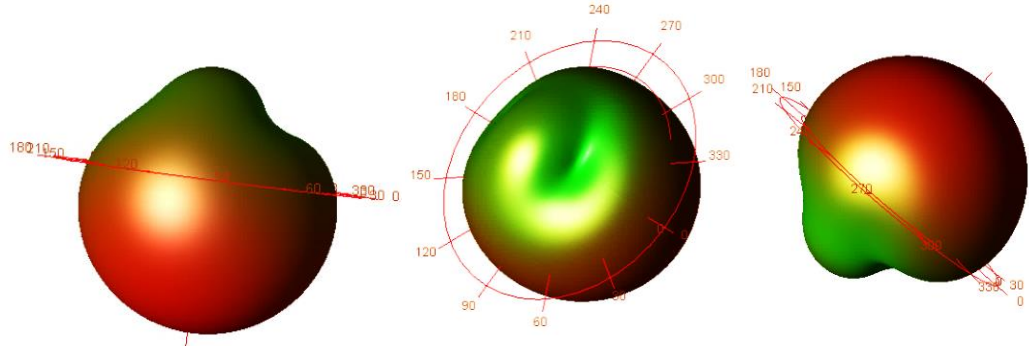


**Fig 4.10 Radiation pattern of the proposed model**

Radiation is the term used to represent the emission or reception of wave front at the antenna, specifying its strength. In any illustration, the sketch drawn to represent the radiation of an antenna is its radiation pattern. One can simply understand the function and directivity of an antenna by having a look at its radiation pattern. Fig. 4.10, shows the radiation pattern of the proposed model.

## **CHAPTER 5**

### **CONCLUSION**

An efficient technique for adding IDLM and back-to-back E-shaped stubs is proposed for MC suppression in micro-strip patch arrays with center-to-center spacing between antenna elements of  $0.5\lambda_0$ . The designed IDLM and E-shaped stub are placed between the H-coupled radiation elements. The influence of coupling elements on the coupling and radiation performance is discussed, and the reason is analyzed through the current and electric field on the antenna. Moreover, the ECC, DG, and TARC of the proposed structure are also studied. The ECC is very small, the DG is large, and the TARC is less than  $-3\text{dB}$ . Owing to the abovementioned features, the proposed structure is a promising candidate for the wireless Rx/Tx or MIMO applications.

## REFERENCE

- [1] P. Garg and P. Jain, “Isolation improvement of MIMO antenna using a novel flower shaped metamaterial absorber at 5.5 GHz WiMAX band,” *IEEE Transactions on Circuits and Systems II: Express Briefs*, vol. 67, no. 4, pp. 675–679, 2021.
- [2] M. Li, L. Jiang, and K. L. Yeung, “Novel and efficient parasitic decoupling network for closely coupled antennas,” *IEEE Transactions on Antennas and Propagation*, vol. 67, no. 6, pp. 3574–3585, 2019.
- [3] B. L. Dhevi, K. S. Vishvaksenan, and K. Rajakani, “Isolation enhancement in dual-band microstrip antenna array using asymmetric loop resonator,” *IEEE Antennas and Wireless Propagation Letters*, vol. 17, no. 2, pp. 238–241, 2018.
- [4] Y.-F. Cheng, X. Ding, W. Shao, and B.-Z. Wang, “Reduction of mutual coupling between patch antennas using a polarization-conversion isolator,” *IEEE Antennas and Wireless Propagation Letters*, vol. 16, pp. 1257–1260, 2017.
- [5] C.-H. Wu, C.-L. Chiu, and T.-G. Ma, “Very compact fully lumped decoupling network for a coupled two-element array,” *IEEE Antennas and Wireless Propagation Letters*, vol. 15, pp. 158–161, 2016.
- [6] R.-L. Xia, S.-W. Qu, P.-F. Li, Q. Jiang, and Z.-P. Nie, “An efficient decoupling feeding network for microstrip antenna array,” *IEEE Antennas and Wireless Propagation Letters*, vol. 14, pp. 871–874, 2015.
- [7] Q. L. Zhang, Y. T. Jin, J. Q. Feng, X. Lv, and L. M. Si, “Mutual coupling reduction of microstrip antenna array using metamaterial absorber,” in

Proceedings of the IEEE MTT-S International Microwave Workshop Series on Advanced Materials and Processes for RF and THz Applications (IMWS-AMP 2020), pp. 1–3, Suzhou, China, July 2015.

- [8] S. Ghosh, T.-N. Tran, and T. Le-Ngoc, “Dual-layer EBG-based miniaturized multi-element antenna for MIMO Systems,” *IEEE Transactions on Antennas and Propagation*, vol. 62, no. 8, pp. 3985–3997, 2014.
- [9] M. M. Bait-Suwailam, O. F. Siddiqui, and O. M. Ramahi, “Mutual coupling reduction between microstrip patch antennas using slotted-complementary split-ring resonators,” *IEEE Antennas and Wireless Propagation Letters*, vol. 9, pp. 876–878, 2010.